



Unleash what's possible.
The guava easyCyte™12 flow cytometer is here.

EMD Millipore is a division of Merck KGaA, Darmstadt, Germany



Functional Gap Junctions Facilitate Melanoma Antigen Transfer and Cross-Presentation between Human Dendritic Cells

This information is current as of May 8, 2015.

Ariadna Mendoza-Naranjo, Pablo J. Saéz, C. Christian Johansson, Marcos Ramírez, Dinka Mandakovic, Cristian Pereda, Mercedes N. López, Rolf Kiessling, Juan C. Sáez and Flavio Salazar-Onfray

J Immunol 2007; 178:6949-6957; ;
doi: 10.4049/jimmunol.178.11.6949
<http://www.jimmunol.org/content/178/11/6949>

References This article **cites 32 articles**, 17 of which you can access for free at:
<http://www.jimmunol.org/content/178/11/6949.full#ref-list-1>

Subscriptions Information about subscribing to *The Journal of Immunology* is online at:
<http://jimmunol.org/subscriptions>

Permissions Submit copyright permission requests at:
<http://www.aai.org/ji/copyright.html>

Email Alerts Receive free email-alerts when new articles cite this article. Sign up at:
<http://jimmunol.org/cgi/alerts/etoc>

The Journal of Immunology is published twice each month by
The American Association of Immunologists, Inc.,
9650 Rockville Pike, Bethesda, MD 20814-3994.
Copyright © 2007 by The American Association of
Immunologists All rights reserved.
Print ISSN: 0022-1767 Online ISSN: 1550-6606.



Functional Gap Junctions Facilitate Melanoma Antigen Transfer and Cross-Presentation between Human Dendritic Cells¹

Ariadna Mendoza-Naranjo,* Pablo J. Saéz,[†] C. Christian Johansson,[‡] Marcos Ramírez,* Dinka Mandaković,* Cristian Pereda,* Mercedes N. López,[§] Rolf Kiessling,[‡] Juan C. Sáez,[†] and Flavio Salazar-Onfray^{2*}

Previously, we found that human dendritic cells (hDCs) pulsed with a melanoma cell lysate (MCL) and stimulated with TNF- α (MCL/TNF) acquire a mature phenotype in vitro and are able to trigger tumor-specific immune responses when they are used in melanoma immunotherapy in patients. In this study, we describe that MCL/TNF induces gap junction (GJ)-mediated intercellular communications and promotes melanoma Ag transfer between ex vivo produced hDCs from melanoma patients. hDCs also exhibit increased expression of the GJ-related protein connexin 43, which contributes to GJ plaque formation after MCL/TNF stimulation. The addition of GJ inhibitors suppresses intercellular tumor Ag transfer between hDCs, thus reducing melanoma-specific T cell activation. In summary, we demonstrate that MCL/TNF-stimulated hDCs can establish functional GJ channels that participate in melanoma Ag transfer, facilitating Ag cross-presentation and an effective dendritic cell-mediated melanoma-specific T cell response. These results suggest that GJs formed between hDCs used in cancer vaccination protocols could be essentials for the establishment of a more efficient antitumor response. *The Journal of Immunology*, 2007, 178: 6949–6957.

Therapeutic vaccines are promising new approaches toward engaging the immune system to target cancer cells. Dendritic cells (DCs)³ are recognized as the most potent APC with the ability to stimulate naive resting T cells and initiate primary immune responses. Since large-scale isolation and expansion of human DCs (hDCs) in cultures have become feasible (1), DC-presenting tumor-associated Ags have been safely administered to cancer patients, inducing significant immunological responses in several clinical trials, including melanoma (2, 3). A phase I clinical study performed in our laboratory for the treatment of advanced malignant melanoma indicates that autologous hDCs obtained from individual patients, pulsed with a melanoma cell

lysate (MCL) and stimulated with TNF- α (MCL/TNF), were able to trigger specific immunological and clinical responses against melanoma-associated Ags (MAA) (4).

DCs are highly interactive cells with extended membrane prolongations that facilitate the interaction among themselves and with other cell types. Previous studies have demonstrated Ag transfer and cross-presentation from living cells to DCs in vitro (5, 6) and in vivo (5, 7). Through such interactions, DCs may acquire Ags even in absence of donor cell apoptosis or necrosis (6), suggesting that processes other than endocytosis are involved. In addition, it has been shown that endogenous DCs play an important role during vaccination with ex vivo produced monocyte-derived DCs, enhancing Ag-specific activation of APC, amplifying Ag presentation, and promoting T cell activation and proliferation (7). These observations indicate that the establishment of interactions between injected and local DCs is essential for an optimal immune response. Recently, it has been reported that activated murine DCs, as well as human monocytes, are able to communicate to each other via gap junctions (GJs) (8, 9).

GJs are clusters of intercellular channels found in the plasma membrane that allow direct intercellular communication between adjacent cells. In mammals, GJ channels are formed by two hexameric hemichannels called connexons, each provided by one of the two contacting cells (10). Connexons are formed by six polytopic trans-membrane protein subunits, termed connexins (Cx), which provide permeability and regulatory properties to the GJ channels (11).

GJ-mediated intercellular communications (GJIC) between murine DCs have been associated to an effective activation by proinflammatory factors such as LPS, TNF- α , and IFN- γ , affecting the DCs' capability to stimulate allospecific T cells (9). Furthermore, it has also been described that human monocytes are capable of transferring and cross-presenting antigenic peptides in a process mediated by GJs (12), indicating a multifunctional role for these membrane structures in the immune response. Besides expression

*Disciplinary Program of Immunology, Institute of Biomedical Sciences, Faculty of Medicine, University of Chile, Santiago, Chile; [†]Department of Physiological Sciences, Faculty of Biological Sciences, Catholic University of Chile, Santiago, Chile; [‡]Department of Oncology and Pathology, Cancer Centre Karolinska, Stockholm, Sweden; and [§]Research Support Office, University of Chile Clinical Hospital, Santiago, Chile

Received for publication November 27, 2006. Accepted for publication March 5, 2007.

The costs of publication of this article were defrayed in part by the payment of page charges. This article must therefore be hereby marked *advertisement* in accordance with 18 U.S.C. Section 1734 solely to indicate this fact.

¹ This work was supported by grants from Fund for the Promotion of Scientific and Technological Development (FONDEF DO211088), National Fund for Scientific and Technological Development (FONDECYT 1060935), Núcleo Milenio de Inmunología e Inmunoterapia P04/030-F, Research Support Office of Clinical Hospital of University of Chile, Swedish Cancer Society (Rolf Kiessling grants), Cancer Society of Stockholm, and European Network for the Identification and Validation of Antigens and Biomarkers in Cancer (Contract 6FP-CT-503306).

² Address correspondence and reprint requests to Dr. Flavio Salazar-Onfray, Disciplinary Program of Immunology, Institute of Biomedical Sciences, Faculty of Medicine, University of Chile, Av. Independencia 1027 Santiago, Chile. E-mail address: Hfsalazar@immunotron.med.uchile.cl

³ Abbreviations used in this paper: DC, dendritic cell; β -Ga, 18 β -glycyrrhetic acid; Cx, connexin; GJ, gap junction; GJIC, GJ-mediated intercellular communication; hDC, human DC; MAA, melanoma-associated Ag; MCL, melanoma cell lysate.

Copyright © 2007 by The American Association of Immunologists, Inc. 0022-1767/07/\$2.00

on murine monocytes and DCs, Cx expression and GJIC have been demonstrated in many other cell types of the immune system (13–16). In this sense, human T cells derived from peripheral blood are able to communicate through GJ channels, and the prevention of interlymphocyte GJIC using GJ inhibitors, such as Cx-mimetic peptides or 18 β -glycyrrhetic acid, results in down-regulation of Ig production *in vitro* (15, 16).

Activation of a specific immune response requires a direct physical interaction between APC and T cells (17). GJ-like structures have also been identified in Langerhans and T cell interfaces both *in vitro* (18) and *in vivo* (19), suggesting a role for these membrane specializations in T cell activation by APC. However, to date there is no evidence demonstrating the existence of GJIC between hDCs and their possible involvement in hDC-Ag transfer and cross-presentation to T cells. In this study, we examined the existence of such interactions in a human melanoma model, using *ex vivo* produced hDCs from melanoma patients. Our results demonstrate functional mechanisms that associate GJIC with Ag transfer/cross-presentation processes and the efficient DC-mediated T cell activation.

Materials and Methods

Patients

PBMC were obtained by leukapheresis, from stage IV melanoma patients included in a previously reported clinical trial (4). The present study was approved by the Bioethical Committee for Human Research of the Faculty of Medicine, University of Chile, and informed written consents were given to and signed by all patients.

Melanoma cell lines and MCL preparation

A MCL derived from a mixture of three allogenic melanoma cell lines, Mel1-3, established at the Institute of Biomedical Sciences, University of Chile, was prepared as follows. The cell lines were obtained from metastatic lymph nodes of HLA-A2⁺ melanoma patients and were positive for the following melanoma-specific markers: MelanA/MART1, S-100, HBM45, A103, 9.2.27, and MC1R (our unpublished data). The cell lines were virus and mycoplasma free. Equal amounts of tumor cells from each cell line were mixed, and the cell pellet was repeatedly frozen and thawed to obtain the MCL, which was then sonicated and irradiated. Protein concentration was calculated by Bradford's method.

Generation of hDCs

Leukocytes were isolated by density gradient separation with Ficoll-Hypaque (Axis-Shield). PBMC (4×10^7 /well) were incubated for 2 h in serum-free AIM-V therapeutic medium (Invitrogen Life Technologies) at 37°C in an atmosphere with 5% CO₂. Nonadherent cells were removed, and the remaining ones were incubated in the presence of human rIL-4 (500 U/ml) (US Biological) and 800 U/ml GM-CSF (Schering-Plough). The cultures were maintained for 7 days, and the medium was replaced every 2 days. At day 6, DCs were treated overnight with 2 ng/ml TNF- α (US Biological) in the presence or absence of MCL (250 μ g/ml).

Dye transfer assays

hDCs were incubated in AIM-V medium alone (Invitrogen Life Technologies) as a control, or stimulated with 2 ng/ml TNF- α , 250 μ g/ml MCL, or both (MCL/TNF), and the functional state of GJ channels between hDCs was tested by observing the transfer of the fluorescent dye Lucifer yellow (Sigma-Aldrich) from a microinjected cell to adjacent cell(s), as described before (9). Microinjection with rhodamine-dextran (Sigma-Aldrich) was used as a negative control. Briefly, the dye (5% w/v Lucifer yellow dilithium salt or rhodamine-dextran in 150 mM LiCl) was microinjected through glass microelectrodes by brief overcompensation of the negative capacitance circuit in the amplifier to cause oscillations until the impaled cell was brightly fluorescent. The cultures were observed on an inverted microscope equipped with xenon arc lamp illumination and a Nikon B filter (excitation wavelength, 450–490 nm; emission wavelength, above 520 nm). At 1 min postinjection, dye transfer was scored. The incidence of dye transfer was also determined for hDCs stimulated with MCL/TNF in the presence of the GJIC inhibitors 18 β -glycyrrhetic acid (β -Ga) (35 or 50 μ M) (Sigma-Aldrich), oleamide (50 μ M) (Sigma-Aldrich), or vehicle only (ethanol) added 15 min before recording. In all experiments, dye transfer

was tested by injecting a minimum of 10 cells. The incidence of dye transfer was calculated as the number of injected cells showing dye transfer to one or more neighboring cells, divided by the total number of cells injected in each experiment multiplied by one hundred.

FACS analysis

hDCs untreated or stimulated with 2 ng/ml TNF- α , 250 μ g/ml MCL, or MCL/TNF were fixed in 2% paraformaldehyde for 15 min. Afterward, washed hDCs were incubated for 30 min on ice in 1% PBS-BSA with the following primary Abs: PE-conjugated anti-human CD11c (eBioscience), FITC-conjugated anti-human CD83, MHC class I, and MHC class II (BD Pharmingen), as well as with the unlabeled primary anti-Cx43 (directed to the C-terminal domain) (20) or anti-Cx45 Ab (directed to the C-terminal domain) (21). For Cx43 and Cx45 analysis, 5-min permeabilization with 0.05% saponin was performed after CD11c-PE primary Ab incubation. For Cx43 and Cx45 analysis, cells were maintained on ice for 30 min with a secondary anti-rabbit FITC-conjugated Ab (Sigma-Aldrich). Controls were conducted in the presence of the secondary anti-rabbit FITC-conjugated Ab (Sigma-Aldrich) alone. Negative controls also included directly labeled isotype-matched irrelevant mAbs. Cells were acquired on a flow cytometer (FACSsort; BD Pharmingen) and analyzed using the CellQuest software.

Western blot

Cell pellets from harvested hDCs that had been untreated or stimulated with TNF- α (2 ng/ml), MCL (250 μ g/ml), or MCL/TNF were suspended at 4°C in ice-cold radioimmunoprecipitation assay buffer plus protease and phosphatase inhibitors. Equal amounts of protein were resuspended in Laemmli 4 \times sample buffer and were separated by 10% SDS-PAGE and visualized with polyclonal anti-Cx43, anti-Cx45 Abs using an ECL system (Amersham Biosciences). As an internal control, a mAb against β -actin (Sigma-Aldrich) was stained for normalization after stripping. The ratio Cx/actin was determined by scanning and quantifying the bands in a Kodak Digital Science 1D 3.0.2 densitometer.

Immunofluorescence staining

hDCs incubated with only medium as control, or stimulated with 2 ng/ml TNF- α , 250 μ g/ml MCL, or MCL/TNF were fixed with cold 70% methanol for 10 min and blocked with 5% BSA-PBS for 1 h. hDCs cultured alone were incubated with the respective primary Abs, as follows: Cx43 and CD11c (Ancell) in 1% BSA-phosphate buffer in humid chamber at 4°C overnight. Protein expression was visualized by incubating the cells with the corresponding secondary fluorescence-conjugated Abs, as follows: goat anti-rabbit FITC conjugated (Sigma-Aldrich) and Alexa Fluor 647 goat anti-mouse (Molecular Probes and Invitrogen Life Technologies) for 1 h. Fluorescence-labeled secondary Abs were added alone as negative controls. Finally, the cells were analyzed by confocal laser scanning microscopy (objective $\times 63$, LSM 510; Carl Zeiss MicroImaging).

Generation of tumor-infiltrating lymphocyte cell line and clones

T lymphocytes were obtained from a fresh pulmonary metastasis of patient MT43 (HLA-A2⁺). After mechanical tissue separation, the resulting single-cell suspension was cultured at 37°C, 5% CO₂ and was fed every 2 days with RPMI 1640 medium supplemented with 10% FBS (Invitrogen Life Technologies) and rIL-2 (375 U/ml) (ProSpec-Tany TechnoGene). At day 14, the CTLs were enriched using CD8 mAb-coupled beads and cloned by limiting dilution in 96-well U-shaped microtiter plates in the presence of feeders (irradiated PBMC from two allogeneic donors, plus rIL-2 (750 U/ml) and 12 μ g/ml OKT-3 mAb). Obtained CTL clones were tested for IFN- γ production against DBF melanoma cell line, HLA-A2⁺, Mart1/MelanA⁺, and against T2 cells pulsed with different MAA peptides derived from proteins Gp100, MC1R, tyrosinase, and MelanA/MART1. The selected clone (CdL43-1) is HLA-A2⁺ restricted and MelanA/MART1_{27–35} specific, and recognizes melanoma cells, as tested by IFN- γ secretion ELISPOT assay.

Cross-presentation assay

HLA-A2⁻ hDCs (5×10^5) were loaded with MCL/TNF (DCA2⁻/MCL) and then washed three times with PBS before a 4-h coinoculation with HLA-A2⁺ hDCs (5×10^5) (DCA2⁺) that had been matured with TNF- α (2 ng/ml) and LPS (1 μ g/ml) in the absence of MCL, and in the presence or absence of 300 μ M 1848 Cx mimetic peptide (95% purity); 300 μ M Gap20 control peptide (95% purity) (JPT Peptide Technology); and 50 μ M β -Ga or 50 μ M oleamide. After incubation, the cell mix was washed three times with PBS and then used as a target (2×10^4 cells/well) in an ELISPOT assay, as described below. The effector cells used were the CdL43-1 MelanA/MART1-specific clone, obtained as described above.

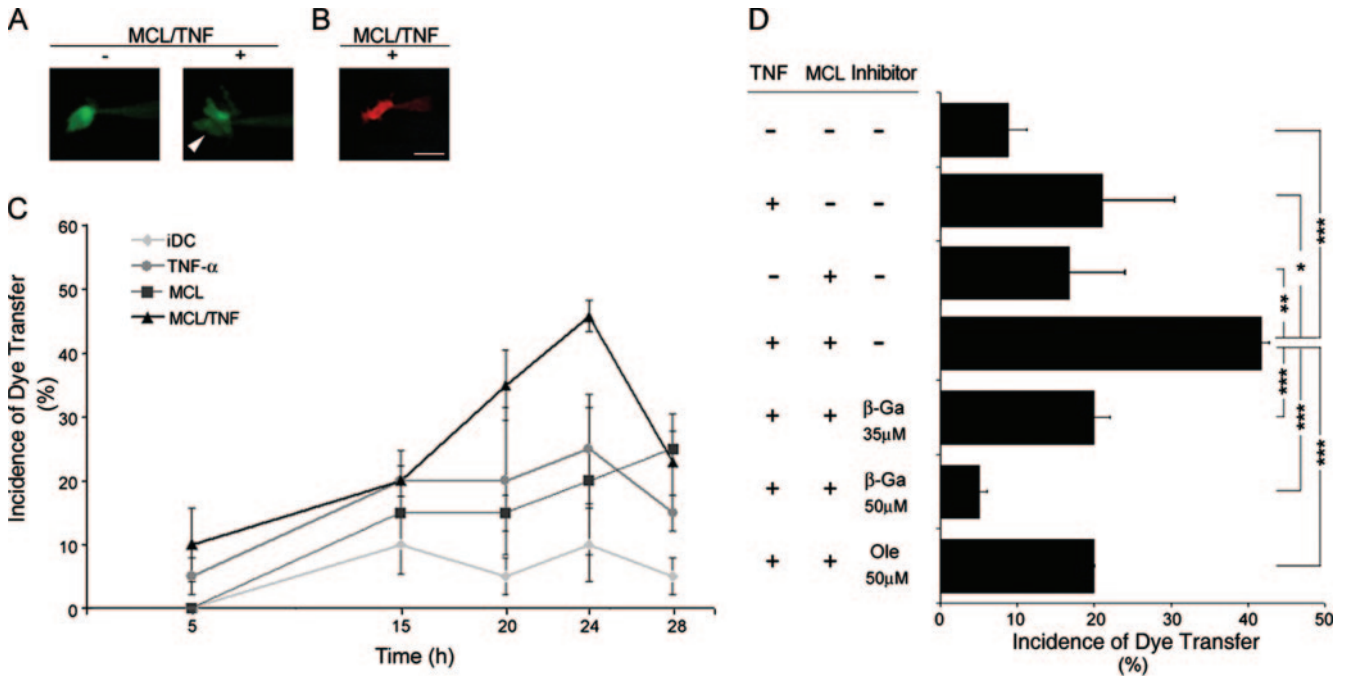


FIGURE 1. MCL/TNF induces dye transfer between hDCs. *A*, Monocyte-derived hDCs were nonstimulated (*left panel*) or stimulated with MCL/TNF for 24 h (*right panel*) and then microinjected with Lucifer yellow. *B*, hDCs treated with MCL/TNF were microinjected with rhodamine-dextran as a negative control. Scale bar = 60 μ m. *C*, The graph shows the incidence of dye coupling measured during a time course for untreated hDCs (diamond), as well as for those stimulated with TNF- α (circle), MCL (square), or MCL/TNF (triangle). Each plotted point represents the mean \pm SEM of four independent experiments. *D*, Untreated hDCs or hDCs stimulated 24 h with TNF- α , MCL, or MCL/TNF were microinjected with Lucifer yellow, and the incidence of dye transfer was measured. GJ channel inhibitors, β -Ga (35 and 50 μ M) and oleamide (50 μ M), were added. Each plotted point represents mean \pm SEM of four independent experiments. Differences in dye transfer incidence are indicated by *p* values, as determined by Student's *t* test (*, *p* < 0.05; **, *p* < 0.01; ***, *p* < 0.005).

Additionally, DCA2⁺ (5×10^5) loaded with MCL/TNF (DCA2⁺/MCL) were cocultured 4 h with DCA2⁻ (5×10^5) and then matured with TNF- α (2 ng/ml) and LPS (1 μ g/ml), in the presence or absence of 300 μ M 1848 peptide, 300 μ M Gap20 control peptide, β -Ga (50 μ M), or oleamide (50 μ M), before IFN- γ ELISPOT assay.

IFN- γ ELISPOT assay

Ninety-six-well MultiScreen plates (MAPN1450; Millipore) were coated overnight with 2 μ g/ml anti-human IFN- γ capture mAb (1-D1K; Mabtech) and then washed and blocked 1 h with RPMI 1640/10% FBS. Cocultures of DCA2⁻/MCL and DCA2⁺, as well as of DCA2⁺/MCL and DCA2⁻, untreated or treated 4 h with GJ inhibitors, as described before, were added in duplicates at 2×10^4 cells/well and cocultured for 15 h at 37°C with Melana/MART1-specific tumor-infiltrating lymphocytes (2×10^3 /well). Unloaded DCA2⁻ and DCA2⁺, as well as DCA2⁻/MCL alone, were used as negative controls. The unspecific background for DCA2⁻/MCL was subtracted in all coculture conditions when it was included. DCA2⁺ matured with MCL/TNF and pulsed with 10 μ g/ml Melana/MART1₂₇₋₃₅ or 10 μ g/ml Gp100₂₀₉₋₂₁₇ peptides were used as positive and negative controls, respectively. IFN- γ spots were detected using 0.5 μ g/ml biotin-conjugated anti-IFN- γ Ab and 0.5 μ g/ml streptavidin-alkaline phosphatase (both from Mabtech), and were counted using an automated ELISPOTscan counter (A.EL.VIS). Results were expressed as the mean of spots/ 2×10^3 effector cells.

Phagocytosis assay

HLA-A2⁺ hDCs (5×10^5), untreated or stimulated with 2 ng/ml TNF- α and 1 μ g/ml LPS for 24 h, were incubated at either 4°C or 37°C with 0.05 μ g/ μ l dextran-FITC for 2 h. Then the cells were rinsed twice with PBS, fixed with 2% paraformaldehyde, and analyzed by FACS (BD Pharmingen).

Statistics

Differences between the compared groups were analyzed by Student's *t* test using Origin software (RockWare). Results were expressed as means \pm SD, or means \pm SEM. Values of *p* < 0.05 were considered statistically significant.

Results

MCL/TNF- α stimulation induces GJIC in hDCs

Activated monocytes and murine DCs are able to communicate to each other via GJ channels (8, 9). To test whether monocyte-derived hDCs could also form functional GJ channels, we analyzed the incidence of dye coupling of hDCs cultured at high density to ensure the establishment of cell-cell contacts allowing GJ channel formation. The intercellular transfer of Lucifer yellow, a fluorescent GJ tracer, was analyzed between untreated hDCs or after stimulation with TNF- α , MCL, or MCL/TNF. The dye transfer incidence was calculated using a confocal microscope, injecting a minimum of 10 DCs per experiment and period of time of interest. The incidence of dye coupling was calculated as percentage by dividing the number of injected cells, showing dye transfer to two or more adjacent cells, by the total number of microinjected cells, and multiplied by 100, as described in *Materials and Methods*.

Under control conditions, hDCs showed a low incidence in dye transfer, remaining often uncoupled (Fig. 1, *A* (*left panel*) and *C*). In contrast, hDCs stimulated with the MCL/TNF mix showed a more frequent dye transfer incidence (Fig. 1, *A* (*right panel*, arrowhead) and *C*). To confirm that Lucifer yellow transfer was only due to GJIC and not due to membrane fusion or formation of cytoplasmic bridges, we also microinjected cells with rhodamine-dextran fluorescent dye in parallel, which is well above (10 kDa) the molecular size permeability limit of GJ channels and thus served as a positive control for GJ-independent pathways. Under all tested conditions, the fluorescence of rhodamine-dextran remained restricted to the microinjected DCs, indicating that intercellular transfer of Lucifer yellow could only occur through GJ channels (Fig. 1*B*).

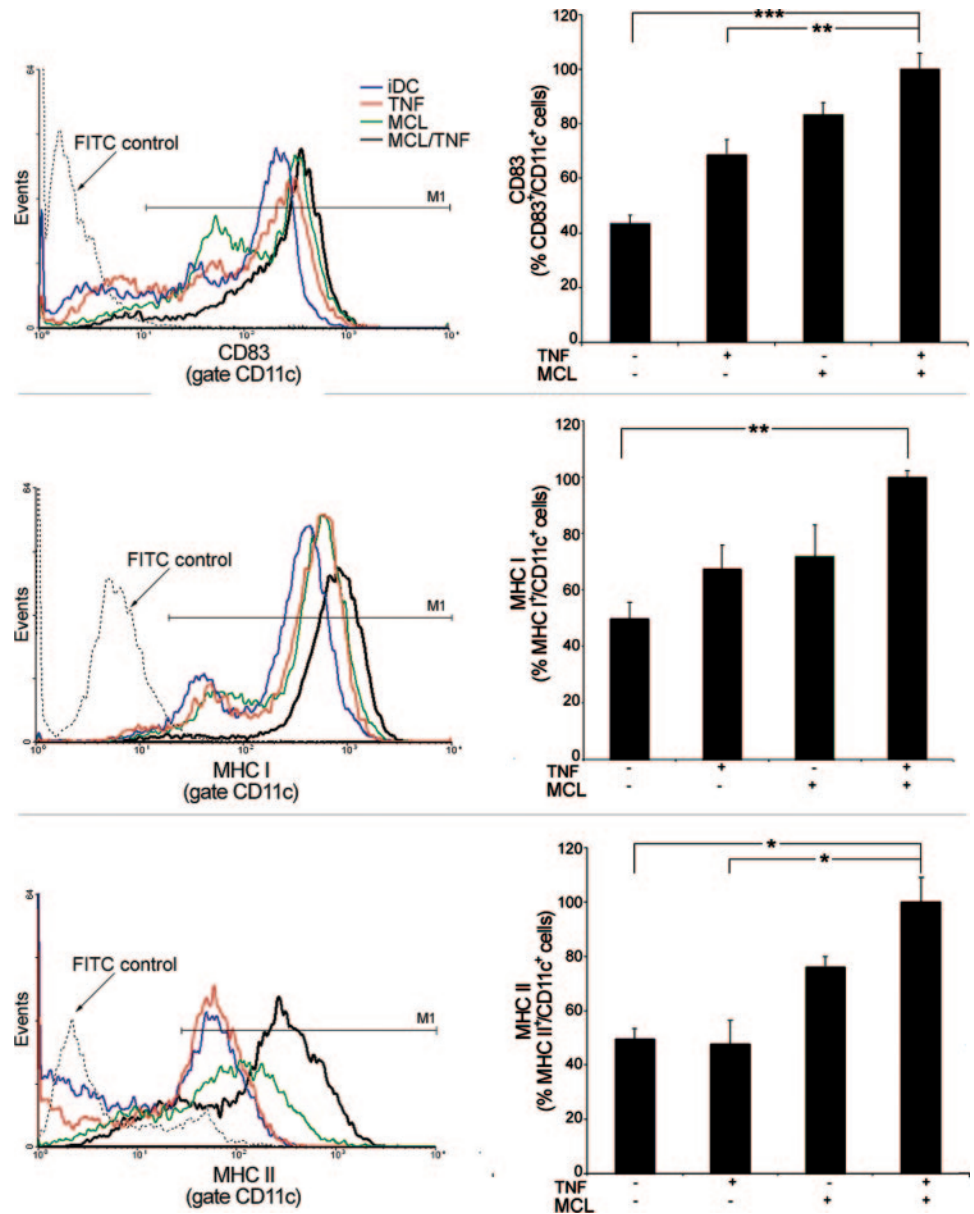


FIGURE 2. MCL/TNF treatment enhances the mature phenotype in hDCs. Nonstimulated immature hDCs (iDCs), as well as immature hDCs stimulated with MCL, TNF- α , or MCL/TNF were tested at different time points for the expression of different cell surface markers by flow cytometry. The expression of CD83, MHC class I, and MHC class II, gated on CD11c, was reported as the percentage of cells positive for these markers within the CD11c⁺ population. Histograms show data of three representative independent experiments. Differences are indicated by *p* values, as determined by Student's *t* test (*, *p* < 0.05; **, *p* < 0.01; ***, *p* < 0.005).

Dye transfer incidence was also detected in DCs subjected to different stimuli for different periods of time (5, 15, 20, 24, and 28 h) (Fig. 1C). A slight enhancement in dye transfer was detected at 20 h between hDCs after the addition of TNF- α , MCL, or MCL/TNF when compared with nonstimulated hDCs (Fig. 1C). The increase of dye transfer was most notable in hDCs treated with MCL/TNF for 24 h, which was significantly higher than the incidence observed in the other studied conditions, including hDCs treated with only TNF- α or MCL (*n* = 4 experiments; *p* < 0.05) (Fig. 1, C and D).

To confirm the GJ involvement in MCL/TNF-mediated dye transfer induction on melanoma patient-derived hDCs, the inhibitory effect of β -Ga and oleamide was investigated. The incidence of dye transfer was studied in hDCs stimulated with TNF- α , MCL, or MCL/TNF in the absence or presence of the GJ inhibitors. Our results show that treatment of hDCs for 24 h with MCL/TNF increased almost 3–4 times (up to 40%) the dye transfer incidence as compared with untreated hDCs, whereas cells treated only with TNF- α or MCL alone showed a nonsignificant difference in the incidence of dye transfer compared with nonstimulated hDCs (Fig.

1D). In contrast, hDCs stimulated with MCL/TNF for 24 h and then treated for 15 min with 35 or 50 μ M β -Ga showed a significant concentration-dependent decrease in the dye transfer incidence that reached ~20 and 5%, respectively (*n* = 3 experiments; *p* < 0.005) (Fig. 1D). Similarly, the presence of 50 μ M oleamide also resulted in a significant (from 40 to 20%; *p* < 0.005) reduction in the dye transfer incidence (Fig. 1D). hDCs treated with MCL/TNF plus ethanol (vehicle of the GJ inhibitors) showed no changes of the dye transfer incidence induced by MCL/TNF (data not shown).

GJIC between DCs have been associated to maturation of murine DCs induced by proinflammatory factors (8). To characterize the maturation state of hDCs at the different experimental conditions, the expression of different surface markers (CD83, MHC class I, and MHC class II) was examined on CD11c-positive cells by flow cytometry. We observed that hDCs stimulated 24 h with MCL/TNF exhibited a more robust mature phenotype than the other studied groups, expressing higher amounts of both MHC class I and class II, as well as the maturation marker CD83 as compared with hDCs at other conditions (Fig. 2). This increased

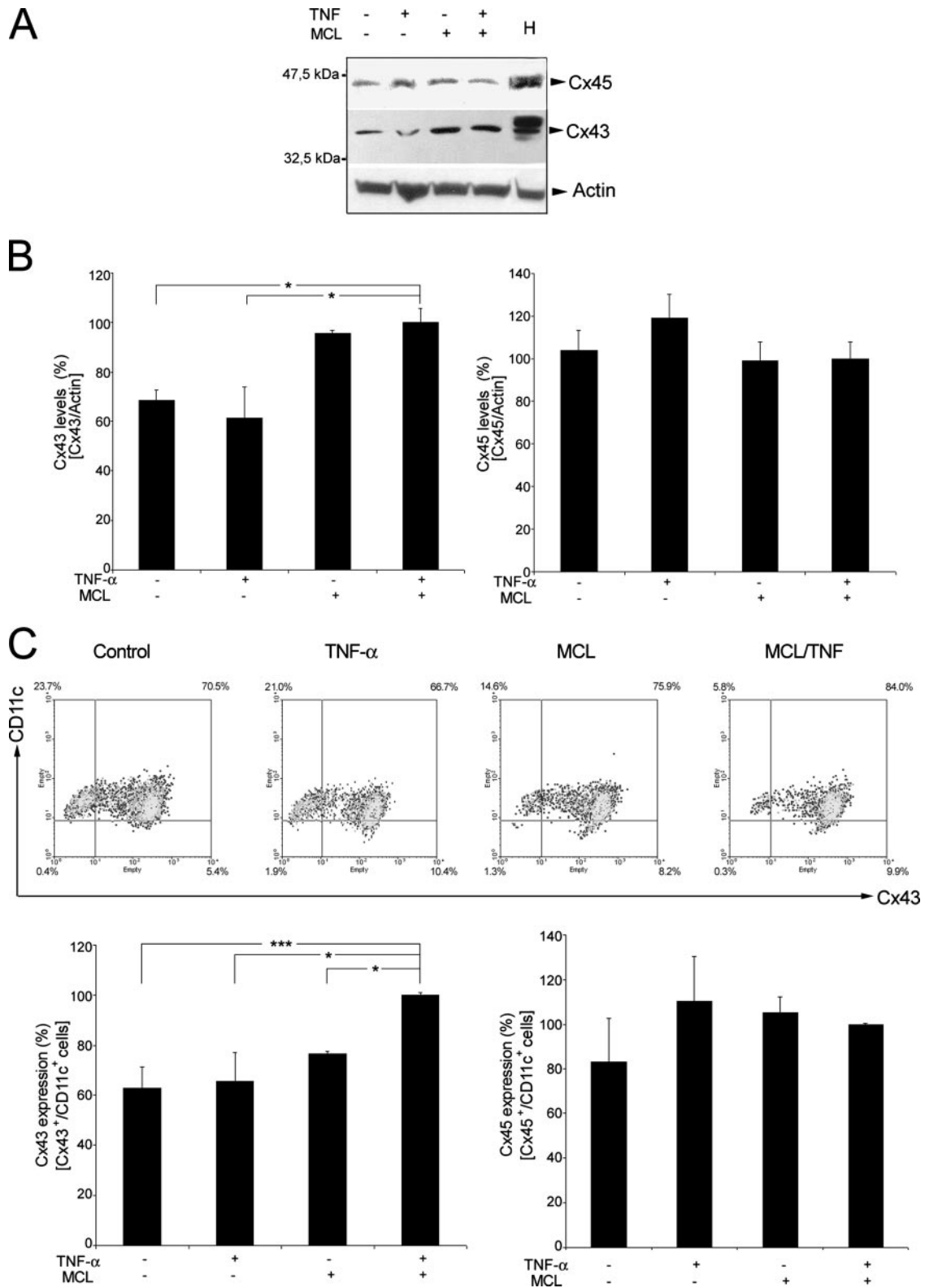


FIGURE 3. MCL/TNF increases Cx43, but not Cx45 levels in hDCs. *A*, Protein extracts were prepared from untreated hDCs, and from hDCs treated with TNF- α , MCL, or MCL/TNF for 24 h. Levels of Cx43 and Cx45 were estimated by Western blot analysis using anti-Cx43- and anti-Cx45-specific Abs. An extract of rat heart was used as a positive control for Cx detection (lane H). *B*, Graphs represent Cx43 and Cx45 levels quantified from the blots by densitometry and normalized against total β -actin levels. Bars represent the mean (percentage) \pm SD of three independent experiments; *, $p < 0.05$. *C*, Nonstimulated hDCs or hDCs stimulated 24 h with TNF- α , MCL, or MCL/TNF were assayed for Cx43 or Cx45 levels within the CD11c⁺ population by flow cytometry. Graphs are representative of three independent experiments and represent Cx43 and Cx45 levels in the CD11c⁺ population, expressed as the percentage of the mean \pm SD; $n = 3$ (*, $p < 0.05$; ***, $p < 0.005$).

mature phenotype observed 24 h after MCL/TNF treatment was concomitant with the maximal incidence of dye coupling found for this condition (Fig. 1, C and D).

Cx43 levels are increased and contribute to GJ plaque formation in MCL/TNF-stimulated hDCs

To assess whether the MCL/TNF-induced increase in dye transfer between hDCs observed at 24 h posttreatment was related to Cx expression in hDCs, Cx43 and Cx45 expression levels were determined by Western blot and flow cytometry (Fig. 3).

Western blot analysis showed that whereas Cx45 expression levels displayed no differences in any of the studied conditions, a significant increase in Cx43 levels was observed in hDCs treated with MCL/TNF compared with nonstimulated hDCs ($n = 4$ experiments; $p < 0.005$) (Fig. 3A). Quantitative analysis of the blots normalized against β -actin, used as a loading control, revealed a Cx43 increase of $\sim 25\%$ ($p < 0.05$) in hDCs stimulated with MCL or MCL/TNF when compared with untreated and TNF-stimulated hDCs (Fig. 3B). Cx43 and Cx45 levels were also determined for the CD11c⁺ population by flow cytometry (Fig. 3C). A significant increase of Cx43 levels of $\sim 30\%$ was observed in hDCs treated with MLC alone or with MLC/TNF, whereas the expression of Cx45 remained stable in all studied conditions (Fig. 3C).

To further verify whether Cxs are involved in the formation of GJ channels responsible for the dye transfer, we performed immunofluorescence experiments to evaluate the cellular distribution of Cx43 in CD11c⁺ hDCs. Cx43 (green)- and CD11c (red)-stained hDCs were examined by confocal microscopy in subconfluent cultures subjected to the different conditions, as follows: nonstimulated (Fig. 4, A–C), and stimulated with TNF- α (Fig. 4, D–F), MCL (Fig. 4, G–I), or TNF/MCL (Fig. 4, J–L). Cx43 was detected in perinuclear regions of the cell body and cell processes in all studied conditions. Interestingly, Cx43 was markedly localized at the plasma membrane of hDCs treated with MCL/TNF (Fig. 4J) and was frequently found at cell-cell contact sites (35% of analyzed cells; $n = 4$ experiments), colocalizing with CD11c, showing a pattern reminiscent of GJ plaques (Fig. 4M, arrowheads). In contrast, TNF-stimulated hDCs, as well as MCL-stimulated hDCs exhibited much less GJ plaque formation (11.3% of analyzed cells for TNF- α and 9.6% for MCL; $n = 4$).

GJIC facilitate MAA transfer and cross-presentation in hDCs

The cross-presentation process facilitated by intercellular peptide transfer mediated by GJIC has been described in the murine model for a carcinoma cell line, as well as for activated monocytes (12). To investigate whether functional GJIC were involved in MAA transfer between hDCs, we analyzed the intercellular transfer of MelanA/MART1 Ag present in the MCL and tested the capacity of the cells that acquire this Ag to trigger a specific T cell response. To this end, HLA-A2-negative hDCs incubated with MCL/TNF (DCA2⁻/MCL) were cocultured with HLA-A2-positive hDCs that had been matured with TNF- α and LPS (DCA2⁺), but without MCL (Fig. 5A). Next, we tested the ability of DCA2⁺ to activate an autologous MelanA/MART1-specific HLA-A2-restricted clone (CdL43-1), obtained from a melanoma patient. All three melanoma cell lines processed to obtain the MCL contain MelanA/MART1 Ag (our unpublished data). Unloaded DCA2⁺ cocultured with DCA2⁻/MCL were able to stimulate IFN- γ secretion by the CdL43-1 clone, but not DCA2⁺ or DCA2⁻ in the absence of MCL, or DCA2⁺ loaded with the gp100_{209–217} peptide (Fig. 5B). To evaluate whether the observed melanoma peptide transfer was mediated by GJIC, the coculture was incubated in the presence of a specific Cx-mimetic peptide. The sequence of this peptide (CNTQQPGCENVCY) corresponds to the extracellular

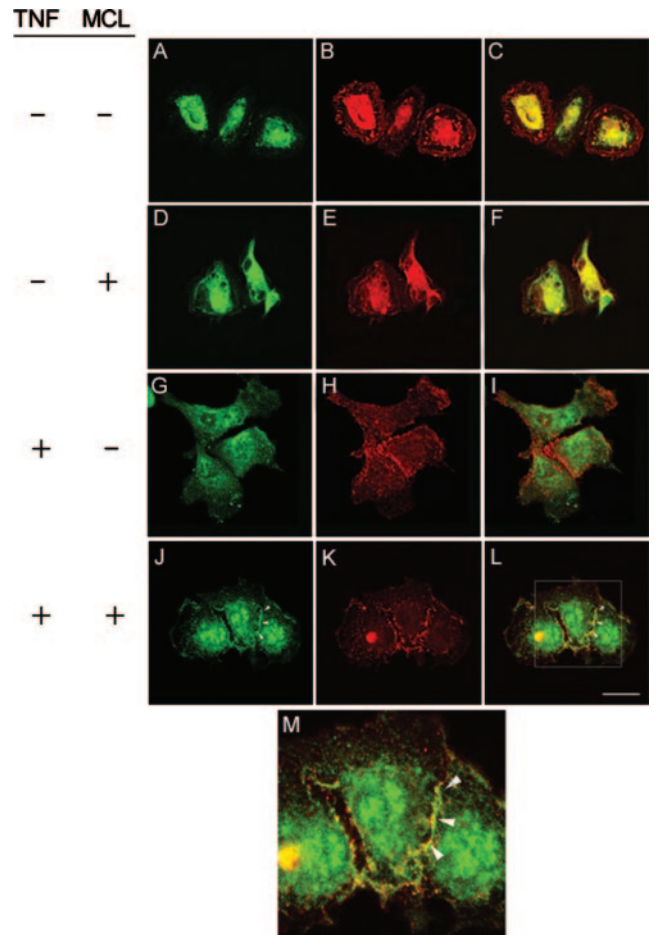
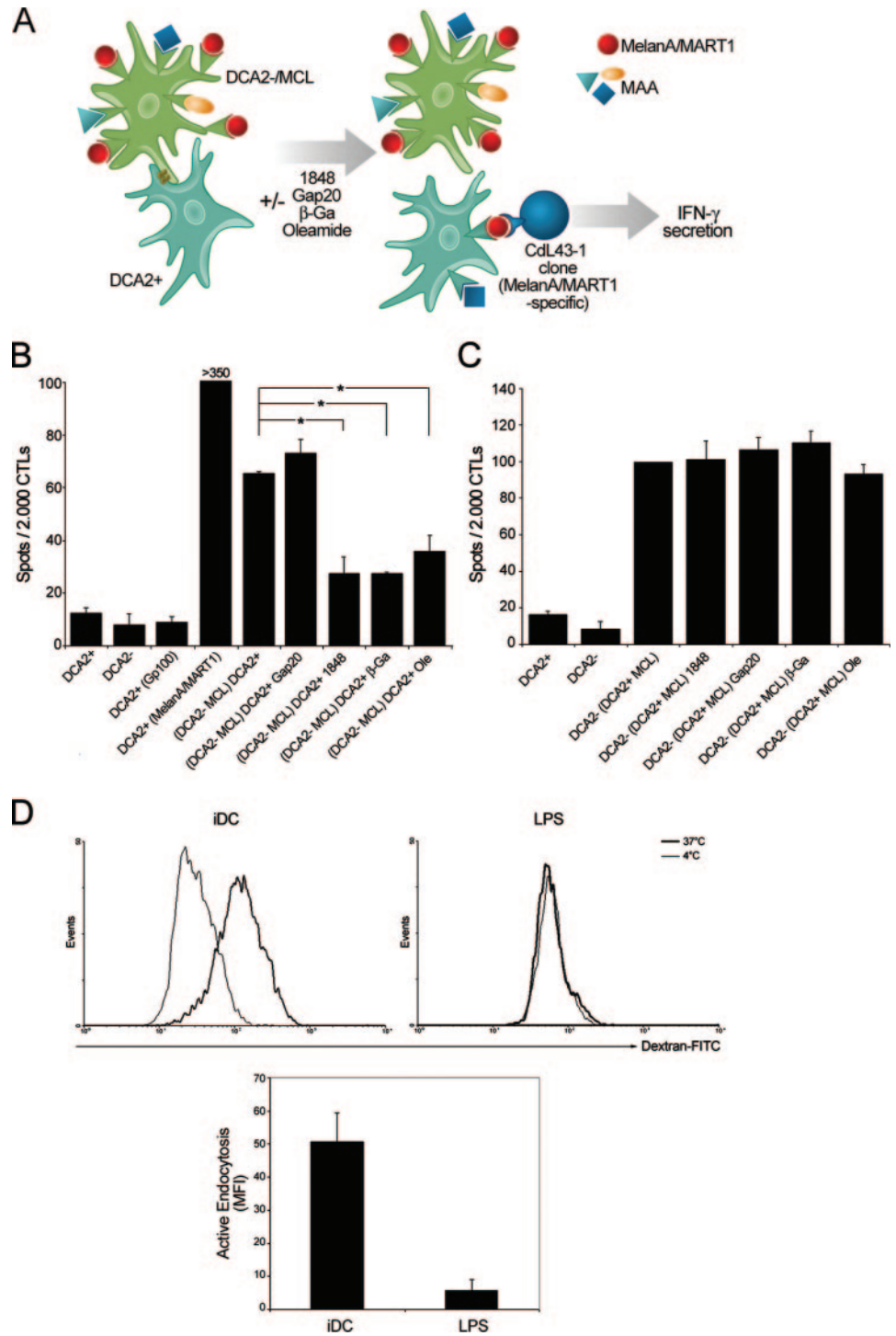


FIGURE 4. Cx43 is localized at cell-cell contacts between hDCs stimulated with MCL/TNF. hDCs treated 24 h with TNF- α (D and E), MCL (G–I), and MCL/TNF (J–L), and nonstimulated hDCs (A–C) were costained for Cx43 (green) and CD11c (red). Confocal microscopy analysis revealed a widespread distribution of Cx43 in CD11c⁺-stained cells for all tested conditions. High power confocal magnification shows Cx43 at cell-cell contacts, colocalizing with CD11c (M; arrowheads). Scale bar = 20 μ m.

loop 1 of Cx43 and is able to block intercellular dye transfer between cells (22). The effect of the two GJ inhibitors, β -Ga and oleamide, was also tested in a similar way. hDCs viability was verified after GJ inhibitor treatment by annexin V/propidium iodide-binding assay, according to the manufacturer's recommendations (BD Pharmingen) (data not shown). The CTL-mediated IFN- γ secretion induced by DCA2⁺ cocultured with DCA2⁻/MCL significantly diminished (50% inhibition) when the hDC mix was cocultured with the 1848 peptide, confirming the participation of Cx43 in Ag transfer between hDCs. Conversely, the presence of the control peptide Gap20 with a sequence corresponding to the intracellular cytoplasmic domain of Cx43 (EIKKFKYGIEEHC) did not affect CTL activation. The addition of GJ blockers β -Ga or oleamide also inhibited Ag transfer, diminishing the capacity of DCA2⁺ to stimulate CTL-mediated IFN- γ secretion (Fig. 5B).

To confirm the specificity of the GJ channel blockers in the intercellular Ag transfer between hDCs, DCA2⁺ loaded with MCL/TNF (DCA2⁺/MCL) were cocultured with DCA2⁻ matured with LPS and TNF- α , in the presence or absence of these inhibitors. DCA2⁺/MCL cocultured with mature DCA2⁻ were able to induce IFN- γ secretion by the CdL43-1 clone, which was not affected by incubation with any of the GJ inhibitors tested, demonstrating the specific effect of these blockers on GJ-mediated Ag

FIGURE 5. Intercellular MAA transfer between hDCs and cross-presentation is inhibited by GJ channel blockers. Transfer assay: *A*, HLA-A2-negative hDCs loaded with MCL/TNF (DCA2⁻/MCL) were cocultured for 4 h in the presence or absence of 1848 inhibitor peptide, Gap20 control peptide, β -Ga, or oleamide, together with the acceptor HLA-A2-positive hDCs matured in the absence of MCL (DCA2⁺). Melanoma Ag transfer was examined using HLA-A2⁺-restricted MelanA/MART1-specific clone (CdL43-1) in an ELISPOT assay. *B*, The cell mixture was used as a target in an IFN- γ ELISPOT assay using CdL43-1 as effector cells. The positive control included mature DCA2⁺ cells loaded with the Melan/MART1 peptide, and untreated DCA2⁺, DCA2⁻, as well as DCA2⁺ loaded with Gp100 were negative controls. *C*, DCA2⁺ loaded with MCL/TNF (DCA2⁺/MCL) were cocultured 4 h in the presence or absence of 1848 inhibitor peptide, Gap20 control peptide, β -Ga, or oleamide, with DCA2⁻ cells matured with TNF/LPS, before the IFN- γ ELISPOT assays. Differences are indicated by *p* values, as determined by Student's *t* test (*, *p* < 0.05). *D*, The phagocytic activity of immature DCA2⁺ (iDC, left panel) and of DCA2⁺ matured with LPS and TNF- α (LPS, right panel) was determined after 2-h incubation with dextran-FITC at 4°C or 37°C. Dextran-FITC uptake was evaluated by flow cytometry. Graphic represents active endocytosis, which was determined by subtracting mean fluorescence intensity values at 37°C minus mean fluorescence intensity at 4°C. Data are representative of two independent experiments and are reported as the mean \pm SD.



transfer, and thus excluding nonspecific effects on Ag presentation or T cell function (Fig. 5C). Additionally, to rule out that Ag uptake was due to GJ-independent phagocytosis, we measured the phagocytic capability of the DCA2⁺ used in the transference assays. Whereas immature DCA2⁺ revealed a strong phagocytic activity at 37°C (Fig. 5D, left histogram), the DCA2⁺ matured with LPS/TNF used in the transference assays showed the same average fluorescence at 37°C as control cells at 4°C (Fig. 5D, right histogram). The graphic shown in Fig. 5D (lower panel) illustrates that whereas immature hDCs possess a high endocytic capability, hDCs matured with LPS/TNF display nearly no phagocytic activity, indicating that Ag transfer in

LPS/TNF-matured hDCs seems not to be mediated by phagocytosis.

Discussion

Tumor-associated Ag-loaded DCs have been proposed as an efficient way to treat cancer patients. The effect of adoptively transferred DCs may be improved by their potential to interact in vivo with local DCs and with other cell types. In this study, we have found that matured hDCs derived from melanoma patients assembled functional GJ channels, allowing direct intercellular communications that facilitate melanoma antigenic transfer and participate in cross-presentation process.

In a recent clinical study, 20 stage IV melanoma patients were immunized with autologous DCs, loaded by using a combination of a MCL and TNF- α (4). In this study, we confirmed that the MCL significantly enhances TNF-mediated induction of DC maturation, which was reflected by the up-regulation of different maturation surface markers. The mechanisms involved in the observed induction of DC maturation remain unclear, and studies to elucidate them are currently underway by members of our group. However, we speculate that membrane-bound molecules or intracellular molecules present in the MCL may act as ligands for TLRs on the DC surface, enhancing the cytokine-mediated maturation signals. It has been described that DC maturation regulates the cross-presentation process in murine DCs (23). In this sense, although immature DCs are capable of accumulating extracellular Ag intended for cross-presentation, presentation will not occur until the cells are activated to mature. Microbial products, cytokines, and physical stimuli are capable of activating Ag processing and presentation on MHC II molecules, but only a subset of these stimuli also facilitated MHC I cross presentation of the same Ag, thus indicating that the exogenous MHC I and MHC II pathways are differentially regulated during DC maturation (23). Additionally, it has been described that the presence of a combination of cytokines may enhance GJ-mediated transfer between DCs (8). In our study, functional GJIC formation in hDCs was markedly increased using MCL/TNF, concomitant with the induction of a more evident mature phenotype. GJIC is a widespread mechanism for the maintenance of homeostasis in tissues and organs, and is essential to coordinate different cellular processes. Although the existence of this type of interaction established between cells of the immune system has been reported previously (8, 9, 13–16), the functional significance of these observations is still poorly understood. GJIC between DCs can occur in response to specific combinations of defined stimulus. In fact, GJIC between DCs was recently described in a murine model, in which the long-term DC line XS52 and also murine bone marrow-derived DCs became effectively dye coupled when activated with LPS or TNF- α plus IFN- γ (8). These observations point to GJ formation as an event associated to DC maturation.

GJ establish pathways of intercellular communication that coordinate processes such as embryogenesis, development, hemopoiesis, growth, and cellular response to injury (22, 24, 25). Individual or combinations of Cx are distributed in cell type-specific patterns, often carrying out specialized functions. In this study, we found that whereas Cx43 and Cx45 are expressed in hDCs, only Cx43 expression was significantly increased further upon MCL/TNF stimulation, in which a systematic increase of Cx43 GJ plaque formation between hDCs was observed. In the immune system, Cx43 is one of the most frequently found proteins related to GJ formation (9, 13–16). In fact, it has been reported that Cx43-GJs functionally couple follicular DCs to each other and to B lymphocytes, in this way participating in direct cell-cell communication in lymphoid germinal centers (14). In addition, Cx43 has also been detected in monocytes, polymorphonuclear cells, activated T cells, and other immune system cell subtypes (12, 13, 15, 16, 22).

We also found that inhibition of GJ formation by using a specific Cx-mimetic peptide that binds to Cx43 extracellular loop 1 at the plasma membrane surface diminished the capability of hDCs to acquire melanoma Ags from adjacent cells and inhibited MAA-specific T cell activation as assessed by IFN- γ production, suggesting a close relationship between Cx43 membrane expression and Ag transfer. In support of this interpretation, we also observed that other traditional GJ inhibitors, β -Ga and oleamide (26, 27), also affected the Ag transfer between hDCs, as well as the antigenic presentation to melanoma-specific T cells.

In general, the induction of a potent antitumor response generated by DC immunization depends on the capability of injected DCs to increase danger signaling in vivo. Our findings describe the participation of GJIC in MAA transfer, providing a better understanding of antigenic transfer mechanisms in hDCs. This opens the possibility of manipulating conditions so as to direct a proper in vivo DC coordination, with the purpose of obtaining an optimal immunization in vaccinated patients. Several studies in murine and human models show that injected DCs are able to activate local DCs and enhance the immune response (2, 3, 28, 29). The interactions between injected and local DCs may occur both in peripheral tissues and also in lymph nodes (7) and may include Ag transfer from DC to DC and a posterior cross-presentation process. Recently, it has been described that activated monocytes can take up antigenic peptides from donor cells through GJIC, and cross-present those peptides in the context of MHC class I to specific T cells (12).

Our present data illustrate that functional GJIC allow melanoma Ag transfer between adjacent hDCs, in which hDCs that acquire MAA through GJs can activate specific CTLs. The involvement of GJs and particularly Cx43 in this process was demonstrated by the inhibition of Ag acquisition after the addition of either a Cx-mimetic peptide or GJ blockers. Although we cannot disregard the participation of other Cxs in the antigenic transfer, the fact that the 1848 Cx43-mimetic peptide inhibits IFN- γ secretion almost to the same extent as β -Ga or oleamide demonstrates the major contribution of this protein to Ag transfer and cross-presentation processes. Although we ensured that Ag transfer could not be mediated by phagocytosis by eliminating all traces of MCL through exhaustive washing before transference assays and by demonstrating that the acceptor mature DCs have a negligible phagocytic activity, we cannot rule out the existence of other possible mechanisms contributing to cross-presentation, such as exosome secretion (30), endoplasmic reticulum-phagosome fusion (31), or FcR γ -mediated cross-presentation (32), among others. However, this GJIC mechanism would allow a very fast and low energy demanding coordination between DCs, facilitating the amplification of antigenic signals, mainly in areas with high cell density, such as lymph nodes.

In summary, our data demonstrate an important role for GJIC between cells of the immune system in a human model that might be relevant from a clinical point of view. In this study, we demonstrate that ex vivo produced hDCs can form functional GJs, allowing both Ag transfer and cross-presentation. These new findings raise new questions regarding the role of this structure in the proper coordination of immune responses and may have a therapeutic potential in a clinical setting regarding cancer therapy.

Acknowledgments

We thank Dr. Tobias Manigold for providing us with the ELISPOTscan counter, and Marisol Briones, Felix González, Manuel Salazar, and Tomas Ohlum for technical help. We also thank Dr. Benedict Chambers for helpful discussions and critical reading of the manuscript.

Disclosures

The authors have no financial conflict of interest.

References

1. Sallusto, F., and A. Lanzavecchia. 1994. Efficient presentation of soluble antigen by cultured human dendritic cells is maintained by granulocyte/macrophage colony-stimulating factor plus interleukin 4 and down-regulated by tumor necrosis factor α . *J. Exp. Med.* 179: 1109–1118.
2. Nestle, F. O., S. Aljagic, M. Gilliet, Y. Sun, S. Grabbe, R. Dummer, G. Burg, and D. Schadendorf. 1998. Vaccination of melanoma patients with peptide- or tumor lysate-pulsed dendritic cells. *Nat. Med.* 4: 328–332.
3. Thurner, B., I. Haendle, C. Roder, D. Dieckmann, P. Keikavoussi, H. Jonuleit, A. Bender, C. Maczek, D. Schreiner, P. von den Driesch, et al. 1999. Vaccination

- with mage-3A1 peptide-pulsed mature, monocyte-derived dendritic cells expands specific cytotoxic T cells and induces regression of some metastases in advanced stage IV melanoma. *J. Exp. Med.* 190: 1669–1678.
4. Escobar, A., M. Lopez, A. Serrano, M. Ramirez, C. Perez, A. Aguirre, R. Gonzalez, J. Alfaro, M. Larrondo, M. Fodor, et al. 2005. Dendritic cell immunizations alone or combined with low doses of interleukin-2 induce specific immune responses in melanoma patients. *Clin. Exp. Immunol.* 142: 555–568.
 5. Inaba, K., S. Turley, F. Yamaide, T. Iyoda, K. Mahnke, M. Inaba, M. Pack, M. Subklewe, B. Sauter, D. Sheff, et al. 1998. Efficient presentation of phagocytosed cellular fragments on the major histocompatibility complex class II products of dendritic cells. *J. Exp. Med.* 188: 2163–2173.
 6. Harshyne, L. A., S. C. Watkins, A. Gambotto, and S. M. Barratt-Boyes. 2001. Dendritic cells acquire antigens from live cells for cross-presentation to CTL. *J. Immunol.* 166: 3717–3723.
 7. Kleindienst, P., and T. Brocker. 2003. Endogenous dendritic cells are required for amplification of T cell responses induced by dendritic cell vaccines in vivo. *J. Immunol.* 170: 2817–2823.
 8. Matsue, H., J. Yao, K. Matsue, A. Nagasaka, H. Sugiyama, R. Aoki, M. Kitamura, and S. Shimada. 2006. Gap junction-mediated intercellular communication between dendritic cells (DCs) is required for effective activation of DCs. *J. Immunol.* 176: 181–190.
 9. Eugenin, E. A., M. C. Branes, J. W. Berman, and J. C. Saez. 2003. TNF- α plus IFN- γ induce connexin43 expression and formation of gap junctions between human monocytes/macrophages that enhance physiological responses. *J. Immunol.* 170: 1320–1328.
 10. Goodenough, D. A. 1975. The structure of cell membranes involved in intercellular communication. *Am. J. Clin. Pathol.* 63: 636–645.
 11. Goodenough, D. A., J. A. Goliger, and D. L. Paul. 1996. Connexins, connexons, and intercellular communication. *Annu. Rev. Biochem.* 65: 475–502.
 12. Neijssen, J., C. Herberts, J. W. Drijfhout, E. Reits, L. Janssen, and J. Neefjes. 2005. Cross-presentation by intercellular peptide transfer through gap junctions. *Nature* 434: 83–88.
 13. Jara, P. I., M. P. Boric, and J. C. Saez. 1995. Leukocytes express connexin 43 after activation with lipopolysaccharide and appear to form gap junctions with endothelial cells after ischemia-reperfusion. *Proc. Natl. Acad. Sci. USA* 92: 7011–7015.
 14. Krenacs, T., M. van Dartel, E. Lindhout, and M. Rosendaal. 1997. Direct cell/cell communication in the lymphoid germinal center: connexin43 gap junctions functionally couple follicular dendritic cells to each other and to B lymphocytes. *Eur. J. Immunol.* 27: 1489–1497.
 15. Oviedo-Orta, E., P. Gasque, and W. H. Evans. 2001. Immunoglobulin and cytokine expression in mixed lymphocyte cultures is reduced by disruption of gap junction intercellular communication. *FASEB J.* 15: 768–774.
 16. Oviedo-Orta, E., T. Hoy, and W. H. Evans. 2000. Intercellular communication in the immune system: differential expression of connexin40 and 43, and perturbation of gap junction channel functions in peripheral blood and tonsil human lymphocyte subpopulations. *Immunology* 99: 578–590.
 17. Springer, T. A. 1990. Adhesion receptors of the immune system. *Nature* 346: 425–434.
 18. Concha, M., A. Vidal, G. Garces, C. D. Figueroa, and I. Caorsi. 1993. Physical interaction between Langerhans cells and T-lymphocytes during antigen presentation in vitro. *J. Invest. Dermatol.* 100: 429–434.
 19. Brand, C. U., T. Hunziker, T. Schaffner, A. Limat, H. A. Gerber, and L. R. Braathen. 1995. Activated immunocompetent cells in human skin lymph derived from irritant contact dermatitis: an immunomorphological study. *Br. J. Dermatol.* 132: 39–45.
 20. Retamal, M. A., C. J. Cortes, L. Reuss, M. V. Bennett, and J. C. Saez. 2006. S-nitrosylation and permeation through connexin 43 hemichannels in astrocytes: induction by oxidant stress and reversal by reducing agents. *Proc. Natl. Acad. Sci. USA* 103: 4475–4480.
 21. Branes, M. C., J. E. Contreras, and J. C. Saez. 2002. Activation of human polymorphonuclear cells induces formation of functional gap junctions and expression of connexins. *Med. Sci. Monit.* 8: 313–323.
 22. Saez, J. C., A. D. Martinez, M. C. Branes, and H. E. Gonzalez. 1998. Regulation of gap junctions by protein phosphorylation. *Braz. J. Med. Biol. Res.* 31: 593–600.
 23. Delamarre, L., H. Holcombe, A. Giodini, and I. Mellman. 2003. Presentation of exogenous antigens on MHC class I and MHC class II molecules is differentially regulated during dendritic cell maturation. *J. Exp. Med.* 198: 111–122.
 24. Rosendaal, M., and C. Jopling. 2003. Hematopoietic capacity of connexin43 wild-type and knock-out fetal liver cells not different on wild-type stroma. *Blood* 101: 2996–2998.
 25. Chanson, M., J. P. Derouette, I. Roth, B. Foglia, I. Scerri, T. Dudez, and B. R. Kwak. 2005. Gap junctional communication in tissue inflammation and repair. *Biochim. Biophys. Acta* 1711: 197–207.
 26. Guan, X., B. F. Cravatt, G. R. Ehring, J. E. Hall, D. L. Boger, R. A. Lerner, and N. B. Gilula. 1997. The sleep-inducing lipid oleamide deconvolutes gap junction communication and calcium wave transmission in glial cells. *J. Cell Biol.* 139: 1785–1792.
 27. Guan, X., S. Wilson, K. K. Schlender, and R. J. Ruch. 1996. Gap-junction disassembly and connexin 43 dephosphorylation induced by 18 β -glycyrrhetic acid. *Mol. Carcinog.* 16: 157–164.
 28. Fields, R. C., K. Shimizu, and J. J. Mule. 1998. Murine dendritic cells pulsed with whole tumor lysates mediate potent antitumor immune responses in vitro and in vivo. *Proc. Natl. Acad. Sci. USA* 95: 9482–9487.
 29. Zitvogel, L., J. I. Mayordomo, T. Tjandrawan, A. B. DeLeo, M. R. Clarke, M. T. Lotze, and W. J. Storkus. 1996. Therapy of murine tumors with tumor peptide-pulsed dendritic cells: dependence on T cells, B7 costimulation, and T helper cell 1-associated cytokines. *J. Exp. Med.* 183: 87–97.
 30. Denzer, K., M. J. Kleijmeer, H. F. Heijnen, W. Stoorvogel, and H. J. Geuze. 2000. Exosome: from internal vesicle of the multivesicular body to intercellular signaling device. *J. Cell Sci.* 113(Pt. 19): 3365–3374.
 31. Guernonprez, P., L. Saveanu, M. Kleijmeer, J. Davoust, P. Van Endert, and S. Amigorena. 2003. ER-phagosome fusion defines an MHC class I cross-presentation compartment in dendritic cells. *Nature* 425: 397–402.
 32. Dhodapkar, K. M., J. Krasovsky, B. Williamson, and M. V. Dhodapkar. 2002. Antitumor monoclonal antibodies enhance cross-presentation of cellular antigens and the generation of myeloma-specific killer T cells by dendritic cells. *J. Exp. Med.* 195: 125–133.